



Universiteit
Leiden
The Netherlands

Pulsar candidates towards Fermi unassociated sources

Frail, D.A.; Mooley, K.P.; Jagannathan, P.; Intema, H.T.

Citation

Frail, D. A., Mooley, K. P., Jagannathan, P., & Intema, H. T. (2016). Pulsar candidates towards Fermi unassociated sources. *Monthly Notices Of The Royal Astronomical Society*, 461, 1062-1067. doi:10.1093/mnras/stw1390

Version: Not Applicable (or Unknown)

License: [Leiden University Non-exclusive license](#)

Downloaded from: <https://hdl.handle.net/1887/47636>

Note: To cite this publication please use the final published version (if applicable).

Pulsar candidates towards *Fermi* unassociated sources

D. A. Frail,¹★ K. P. Mooley,²★† P. Jagannathan^{1,3} and H. T. Intema⁴

¹National Radio Astronomy Observatory, 1003 Lopezville Road, Socorro, NM 87801, USA

²Astrophysics, Department of Physics, University of Oxford, Keble Road, Oxford OX1 3RH, UK

³Department of Astronomy, University of Cape Town, Private Bag X3, Rondebosch 7701, Republic of South Africa

⁴Leiden Observatory, Leiden University, Niels Bohrweg 2, NL-2333 CA Leiden, the Netherlands

Accepted 2016 June 7. Received 2016 June 6; in original form 2016 March 24

ABSTRACT

We report on a search for steep spectrum radio sources within the 95 per cent confidence error ellipses of the *Fermi* unassociated sources from the Large Area Telescope (LAT). Using existing catalogues and the newly released Giant Metrewave Radio Telescope all-sky survey at 150 MHz, we identify compact radio sources that are bright at MHz frequencies but faint or absent at GHz frequencies. Such steep spectrum radio sources are rare and constitute a sample of pulsar candidates, selected independently of period, dispersion measure, interstellar scattering and orbital parameters. We find point-like, steep spectrum candidates towards 11 *Fermi* sources. Based on the gamma-ray/radio positional coincidence, the rarity of such radio sources, and the properties of the 3FGL sources themselves, we argue that many of these sources could be pulsars. They may have been missed by previous radio periodicity searches due to interstellar propagation effects or because they lie in an unusually tight binary. If this hypothesis is correct, then renewed gamma-ray and radio periodicity searches at the positions of the steep spectrum radio sources may reveal pulsations.

Key words: catalogues – surveys – pulsars: general – gamma-rays: general – radio continuum: general.

1 INTRODUCTION

The *Fermi* mission ushered in a golden era in the study of neutron stars, rich in both observational and theoretical developments (Caraveo 2014). There are currently more than 170 gamma-ray pulsars known, and the pace of new discoveries continues unabated. In the Second LAT Pulsar gamma-ray catalogue (2PC; Abdo et al. 2013) one-third are millisecond pulsars (MSPs) distributed isotropically on the sky, while the remainder are normal, mostly young pulsars concentrated in the Galactic plane. Approximately half of the pulsars (PSRs) in the 2PC are *new* discoveries, found by searching for pulsations towards the unassociated LAT sources (Acero et al. 2015). Such searches are either blind, based on the gamma-ray photons alone (e.g. Pletsch et al. 2012a), or are guided by the initial detections and timing ephemerides from radio wavelengths (Ransom et al. 2011).

While the yield has been high, there are still many more pulsar-like candidates among the *Fermi* LAT unassociated sources towards which no radio pulsations have been found, especially at low galactic latitudes. Camilo et al. (2012) argue that most of radio pulsars in the Galactic plane that can be found by current telescopes have already been found by past large area surveys and that the lack of radio

pulsations among these unassociated sources is because the radio beams are not pointed along our line of sight. There is some support for this hypothesis since the majority of blindly detected gamma-ray pulsars are not strong radio emitters. Formally, these so-called radio-quiet pulsars are defined as having a phase-averaged flux density at 1.4 GHz $S_{\nu} < 30 \mu\text{Jy}$. However, a pulsar could still be radio bright but its detection via a radio periodicity search could also be thwarted by the effects of scattering, dispersion, and/or absorption, either along the line of sight or in the immediate environment of the pulsar. In these cases a radio imaging approach may be useful by identifying compact, steep spectrum radio sources.

Historically, new pulsar classes such as isolated millisecond pulsars (Rickard & Cronyn 1979; Erickson 1980) and globular cluster pulsars (Hamilton, Helfand & Becker 1985) have been initially identified this way, as well as unusual young or luminous millisecond pulsars (Strom 1987; Navarro et al. 1995) have been initially identified through the radio imaging approach via their steep spectra. Here, we advocate this approach in order to identify pulsar candidates towards the unassociated sources from the Large Area Telescope (LAT) from *Fermi*. While radio spectra are routinely used in identifying promising blazar candidates (e.g. Massaro, Thompson & Ferrara 2015), this is the first time, to the best of our knowledge, that the method is used for LAT pulsar candidates.

In this paper, we use the recently completed Giant Metrewave Radio Telescope (GMRT) 150 MHz All-Sky Radio Survey (TGSS ADR; Intema et al. 2016) to identify new pulsar candidates towards

* E-mail: dfrail@nrao.edu (DAF); kunal.mooley@physics.ox.ac.uk (KPM)

† Hintze Research Fellow.

Table 1. Steep spectrum radio sources towards *Fermi* unassociated sources.

RA	DEC	l, b	S_t	S_p	α	3FGL name	Sig.	Curv.	Var.	Λ
02:58:38.62 (± 0.02)	+05:51:51.0 (± 0.4)	170.7, -44.9	135.3 ± 7.3	129.6 ± 4.3	-2.05	J0258.9+0552	8.0	1.72	38.9	740
15:33:55.36 (± 0.04)	-52:32:58.3 (± 3.3)	326.3, +2.8	157.5 ± 12.8	133.2 ± 6.5	-1.89	J1533.8-5231	6.4	1.80	50.0	21 300
16:39:23.83 (± 0.03)	-51:46:34.1 (± 2.8)	334.2, -3.3	174.9 ± 16.3	169.3 ± 7.7	-1.95	J1639.4-5146	20.1	1.85	58.0	43 900
17:47:00.24 (± 0.06)	-35:05:54.2 (± 1.9)	354.9, -3.4	78.7 ± 15.6	90.0 ± 8.3	-1.77	J1747.0-3506	11.7	1.85	64.5	41 300
18:27:36.25 (± 0.03)	-08:49:41.3 (± 0.6)	22.4, +1.2	229.9 ± 13.8	196.2 ± 8.3	-2.02	J1827.6-0846	8.7	1.42	51.6	1700
18:30:38.71 (± 0.11)	-31:35:03.9 (± 3.2)	2.4, -9.8	79.6 ± 11.6	56.9 ± 7.3	-1.53	J1830.8-3136	5.3	2.42	40.9	1700
19:01:33.72 (± 0.02)	-01:25:28.0 (± 0.3)	32.8, -2.9	361.8 ± 14.7	329.2 ± 8.8	-2.23	J1901.5-0126	14.0	1.59	60.4	22 000
19:25:33.03 (± 0.14)	+17:22:36.1 (± 1.6)	52.2, +0.6	74.7 ± 10.4	49.7 ± 6.8	-1.52	J1925.4+1727	9.6	6.29	47.3	400
19:49:04.82 (± 0.07)	+24:32:34.4 (± 1.1)	61.2, -0.7	160.4 ± 11.4	99.5 ± 7.6	-1.51	J1949.3+2433	8.2	5.00	42.2	1600
20:28:24.33 (± 0.05)	+40:37:49.8 (± 0.6)	79.1, +1.1	389.7 ± 20.2	292.6 ± 12.6	-1.57	J2028.5+4040c	5.0	3.71	48.8	5500
22:11:08.27 (± 0.05)	+59:25:43.9 (± 0.3)	103.8, +2.6	158.7 ± 5.0	121.9 ± 3.2	-1.71	J2210.1+5925	9.7	2.46	54.9	320

Notes: (a) RA and DEC quote Gaussian fit errors only. An extra uncertainty of 1.55 arcsec should be added in quadrature to these fit errors in order to obtain the true (1σ) astrometric error for the TGSS ADR survey.

Fermi unassociated sources. This paper is arranged as follows. In Section 2 we outline our search methods, while in Section 3 we describe the properties the compact, steep spectrum radio sources. We end in Section 4 summarizing the evidence that these are pulsar candidates and we outline the next steps needed to confirm.

2 METHODS

2.1 The GMRT 150 MHz All-Sky Radio Survey

Between 2010 April and 2012 March the Giant Metrewave Radio Telescope carried out a continuum survey at 150 MHz covering approximately 37 000 deg², or 90 per cent of the sky down to a declination of -53° . The survey achieves a median rms noise level of 3.5 mJy beam⁻¹, with an approximate resolution of 25 arcsec. The measured overall astrometric accuracy is better than 1.55 arcsec in RA and DEC (1σ), while the flux density accuracy is conservatively estimated at ~ 10 per cent. The data are publicly available online¹ in the form of $5^\circ \times 5^\circ$ mosaicked images, image cutouts at user-specified locations, or in the form of a catalogue of 0.63 million radio sources. For more details about the TGSS ADR we refer the reader to Intema et al. (2016).

2.2 The 3FGL unassociated sources sample

One-third of all sources in the gamma-ray sky have no firm counterparts at other wavelengths and they are designated as ‘unassociated’ sources. In the recent third *Fermi* LAT source catalogue (3FGL) there are 3033 discrete sources (Acero et al. 2015). Active galactic nuclei (AGN), mainly blazars, dominate the known sample (57 per cent), followed by single and binary pulsars (6 per cent), with supernova remnants, pulsar wind nebulae and other Galactic objects as the next most common sources class. Unassociated sources are the second-most populous source classification. There are 1010 unassociated sources in the 3FGL catalogue or 33 per cent of the known gamma-ray sources. 839 of these are above the declination cutoff of TGSS ADR of Dec $> -53^\circ$.

Using TOPCAT (Taylor 2005), we searched the TGSS ADR catalogue for all 150 MHz radio sources within the 95 per cent confidence error ellipses of all *Fermi* unassociated sources. Following Petrov et al. (2013), we adjusted the size of the major and minor axes of the 95 per cent error ellipses ($\theta_{\text{maj}}, \theta_{\text{min}}$) that are published in the 3FGL in order to reflect the true 3σ distribution as determined

empirically from the distribution of position offsets of radio and *Fermi* gamma-ray AGN. For the 3FGL (2FGL) this amounts to a factor of 1.148 (1.096) (F. Schnitzel, private communication).

We detected 1485 TGSS ADR sources towards 492 *Fermi* regions. A two-point radio spectral index was derived for all 1485 sources at 150 MHz by cross-matching them with the 1.4 GHz NRAO VLA Sky Survey above Dec $\geq -40^\circ$ (NVSS; Condon et al. 1998) and the 843 MHz Sydney University Molonglo Sky Survey (SUMSS; Bock, Large & Sadler 1999) for Dec $< -40^\circ$. For the TGSS ADR sources, with neither an NVSS nor an SUMSS counterpart, we calculated a lower limit on the spectral index using based on the sensitivity limit of these surveys. An initial candidate list of 25 steep spectrum sources was identified from the original 1485 by requiring $\alpha \leq -1.50$. We further whittled down this list through a visual inspection of the TGSS ADR images and any other archival radio images at other wavelengths. Apart from the aforementioned NVSS and SUMSS, we used radio images from the Faint Images of the Radio Sky at Twenty centimeters survey (FIRST; Becker, White & Helfand 1995) at 1.5 GHz, the Westerbork Northern Sky Survey (WENSS; Rengelink et al. 1997) at 326 MHz, and the Very Large Array Low-frequency Sky Survey Redux (VLSS; Lane et al. 2014) at 74 MHz. In this manner we were able eliminate extended, steep spectrum sources and flag suspicious candidates in confused regions as possible imaging artefacts.

Our final list of 11 compact, steep spectrum candidates is listed Table 1. For each radio source we give the best-fitting TGSS ADR position (J2000), its Galactic longitude and latitude, the total flux density (S_t) and peak flux (S_p) at 150 MHz with errors, and a spectral index (α). For those sources detected in more than two radio sky surveys, we revised the original two-point spectral index (α) with a simple least squares fit to a power law. The errors on α are at least 15 per cent. The real uncertainty is likely larger and results from the fact that the flux densities used in estimating α are taken from surveys whose measurements were made often decades apart (see Section 4).

Each radio source also has accompanying 3FGL information taken from the catalog that includes the 3FGL designation, and the measures of the significance of the gamma-ray detection (Sig.) spectral curvature (Curv.) and the variability (Var.). Finally, for each radio source we estimate a likelihood ratio (Λ). This ratio is defined as the probability that the position offset between the radio and gamma-ray source is due to statistical error (i.e. a Rayleigh distribution) divided by the probability that the radio source is a background radio source unrelated to the *Fermi* source (Schinzel et al. 2015). The numerator requires an estimate of the normalized

¹ <http://tgssadr.strw.leidenuniv.nl/>

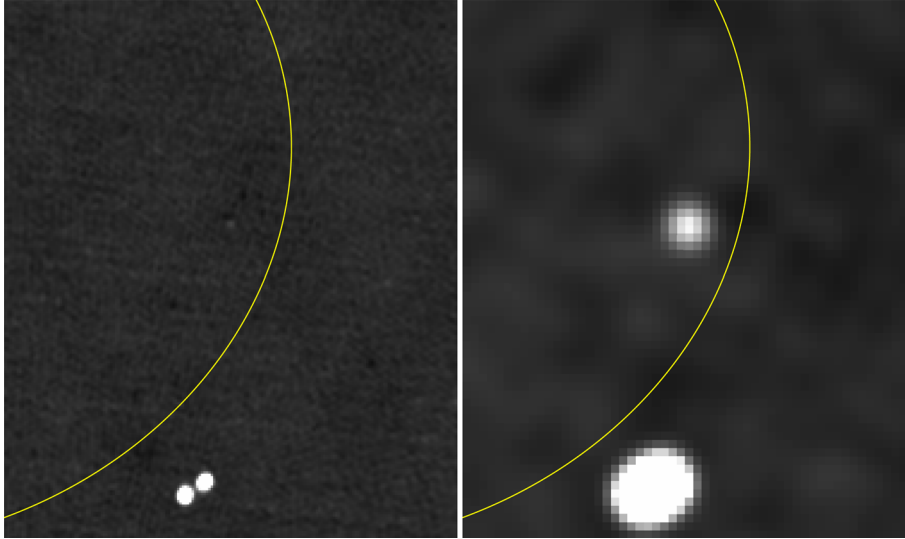


Figure 1. Right: a steep spectrum pulsar candidate towards 3FGL J0258+0552 with a low likelihood ratio (Δ) in the centre of the TGSS ADR image at 150 MHz (135 mJy) shown here with the original *Fermi* error ellipse (yellow line). On the left is a FIRST image at 1.4 GHz showing a faint (1.2 mJy) and unresolved point source. The field of view is $6.7 \text{ arcmin} \times 5.6 \text{ arcmin}$ and the rms noise in the FIRST and TGSS ADR images are 0.15 and $3.6 \text{ mJy beam}^{-1}$, respectively.

offset of the radio source from the centre of the *Fermi* ellipse. The denominator requires that we know the number of steep spectrum radio sources within a circle of radius equal to the angular separation between the *Fermi* source and the TGSS ADR source. At the completeness limit of the TGSS ADR, there are approximately 17 sources per square degree but we note in Intema et al. (2016) that only about 10 per cent of these sources are steep spectrum (i.e. $\alpha < -1.59$), or 1.7 deg^{-2} .

2.3 The empty 2FGL fields

Schinz et al. (2015) have produced a catalogue of compact radio sources at 5 and 9 GHz towards *all* of the 2FGL *Fermi* unassociated sources. After accounting for the newly found associations, they find that 117 of these gamma-ray sources have no compact radio candidate to the detection limit (1–2 mJy) of their survey. Following the identical method as in Section 2.2 we found 129 TGSS ADR sources within the 95 per cent confidence interval of 42 of these 2FGL sources. There is a similar number of NVSS and SUMSS radio sources within these same regions. Suffice to say, these fields are only ‘empty’ in the sense that they lack compact radio sources at 5 and 9 GHz.

We identified three steep spectrum candidates using the same method as above. Two of these are already in our Table 1 and have 3FGL counterparts. These are 2FGL J1827.4–0846 and 2FGL J1639.8–5145. A third candidate inside the 2FGL J0955.0–3949 error ellipse is a weak point source in TGSS ADR (77 mJy) but lies in fields where the SUMSS and NVSS are noisy and thus the spectral index ($\alpha = -1.6$) estimate is highly uncertain. It lies on the edge of the 95 per cent 2FGL error ellipse but it falls outside of the improved 3FGL error circle. For this reason, we do not consider this a viable candidate.

3 PULSAR CANDIDATES

Using the method described in Section 2, we found 11 pulsar candidates. We also found one known pulsar, PSR B1848+04, hitherto not claimed to be associated with any *Fermi* source. This is an old,

normal pulsar with a period of 284 ms that lies within the *Fermi* unassociated source 3FGL J1851.2+0423. In this section, we give a brief description about the properties of each candidate and explore the possible multiwavelength counterparts of these candidates.

There are a number of optical-infrared associations for the majority of the candidates, but given their current positional accuracy of a few arcseconds and the proximity to the Galactic plane, the high optical source densities in these regions make it difficult to identify counterparts with certainty. X-ray observations have been undertaken by the *Swift* satellite towards seven of our 3FGL regions² (Stroh & Falcone 2013). The integration times varied from 0.1 to 7 ks. We also additionally checked the latest all-sky catalogues of the *ROSAT*, *Chandra*, and *XMM-Newton* telescopes. There are no detections of X-ray sources coincident with any of our radio candidates.

3.1 3FGL J0258.9+0552

This candidate has a peak flux density of $129.6 \pm 4.3 \text{ mJy beam}^{-1}$ at 150 MHz, and the spectral index between 150 MHz and 1.4 GHz is -2.05 . There is a weak detection of this source in FIRST and NVSS images. The former allows us to improve the position and angular resolution. The FIRST source is unresolved at 1.4 GHz with a synthesized beam of 5 arcsec, $S_{\text{t}} = 1.21 \pm 0.22 \text{ mJy}$, and $S_{\text{p}} = 1.45 \pm 0.14 \text{ mJy beam}^{-1}$. This allows precise localization of the candidate, RA = $02^{\text{h}}58^{\text{m}}38^{\text{s}}.56$, DEC = $05^{\circ}51'52''.8$, with uncertainties of 0.2 arcsec in both coordinates. At this location, there are no viable multiwavelength counterparts in the Vizier data base. We show the FIRST and TGSS ADR images in Fig. 1.

3.2 3FGL J1533.8–5231

This candidate has a strong detection in TGSS ADR ($S_{\text{t}} = 157.5 \pm 12.8 \text{ mJy}$), but only an upper limit in the SUMSS catalogue. At the location of the TGSS source, the peak pixel value in the

² The results are available online at <http://www.swift.psu.edu/unassociated/>.

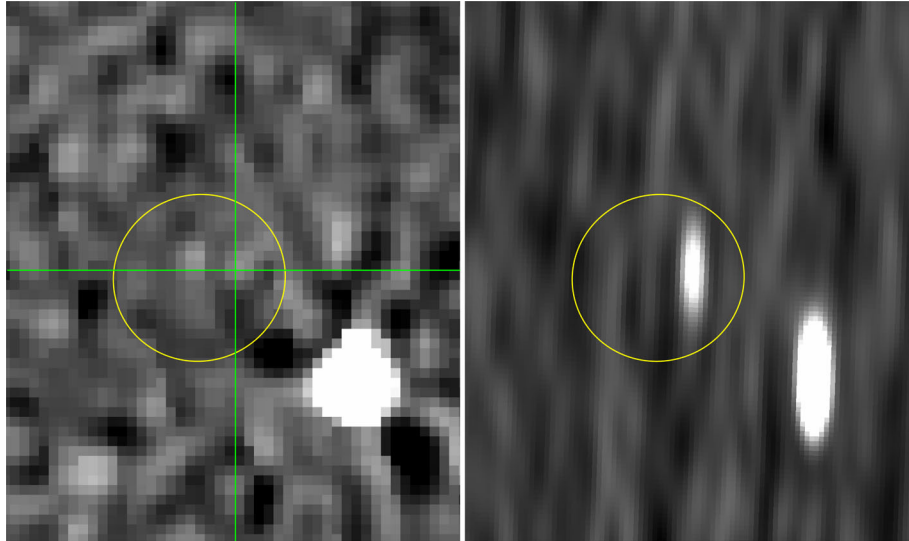


Figure 2. Right: a steep spectrum pulsar candidate towards 3FGL J1639.4–5146 with a high likelihood ratio (Δ) in the centre of the TGSS ADR image at 150 MHz (175 mJy) shown here with the original *Fermi* error ellipse (yellow line). On the left is a SUMSS image at 843 MHz with (green) cross-hairs indicating a faint, uncatalogued radio source (<3 mJy) at the same position as the 150 MHz source. The field of view is $11.9 \text{ arcmin} \times 9.2 \text{ arcmin}$ and the rms noise in the SUMSS and TGSS ADR images are 1.3 and $9.8 \text{ mJy beam}^{-1}$, respectively.

SUMSS is 1.6 mJy , implying that the spectrum is slightly steeper than that given in the Table 1, -1.89 . There are no multiwavelength counterparts within 5 arcsec of the TGSS ADR source in the Vizier data base.

3.3 3FGL J1639.4–5146

The 3FGL error circle is small ($\theta_{\text{maj}} = 2 \text{ arcmin}$) and it has a bright ($S_{\text{t}} = 174.9 \pm 16.3 \text{ mJy}$), compact TGSS ADR source within it. There is no catalogued SUMSS counterpart for the TGSS ADR source, but at that location the peak pixel value in SUMSS is $2.9 \text{ mJy beam}^{-1}$. Thus, the spectral index in Table 1, -1.95 , is an upper limit. A possible optical counterpart with a *B* band magnitude of 18.8 is catalogued in USNO-B1.0, and is located 2.1 arcsec from the TGSS ADR source. We show the SUMSS and TGSS ADR images in Fig. 2.

3.4 3FGL J1747.0–3506

A point-like TGSS ADR source with $S_{\text{t}} = 78.7 \pm 15.6 \text{ mJy}$ lies in the centre of the 3FGL error ellipse ($\theta_{\text{maj}} = 6 \text{ arcmin}$). There are no NVSS or SUMSS counterparts at this location at the level of $>1 \text{ mJy beam}^{-1}$. Based on this upper limit, we derive an upper bound of -1.77 to the spectral index between 150 MHz and 1.4 GHz . We note that there is some extended emission just NW, offset by 1 arcmin , from this location in NVSS, which is likely unrelated to the TGSS ADR source. There are various possible optical counterparts having *V*-band magnitudes of ~ 20 located within 2.5 arcsec catalogued in Vizier data base.

3.5 3FGL J1827.6–0846

This candidate is on the edge of the 3FGL error circle, and has a total flux density of $229.9 \pm 14.8 \text{ mJy}$ in TGSS ADR. There is no NVSS emission at this location at a level of $<0.8 \text{ mJy beam}^{-1}$, but there is a $777 \pm 126 \text{ mJy}$ VLSS_r source. This confirms the steep spectrum nature of the TGSS ADR source. The spectral index

between 150 MHz and 1.4 GHz is therefore less than -2.0 , while between 74 MHz and 150 MHz it is approximately -2.6 . There are two possible counterparts in UKIDSS located $\sim 1.3 \text{ arcsec}$ from the TGSS ADR location.

3.6 3FGL J1830.8–3136

The density of the TGSS ADR source is $79.6 \pm 11.6 \text{ mJy}$. At this position, the NVSS registers a weak source, possibly extended with $S_{\text{t}} = 2.6 \pm 0.5 \text{ mJy}$ and $S_{\text{p}} = 0.96 \pm 0.55 \text{ mJy beam}^{-1}$. Inspection of the NVSS image cutout suggests that this could be a sidelobe of a brighter, 54 mJy , source located to the SW. There is only an upper limit with SUMSS of $<3.5 \text{ mJy beam}^{-1}$. The spectral index between 150 MHz and 1.4 GHz derived assuming 2.6 mJy flux density in NVSS is -1.53 . There are no other counterparts within 5 arcsec of the TGSS ADR source in the Vizier data base.

3.7 3FGL 1901.5–0126

This candidate is detected (strongly, with $S_{\text{t}} = 361.8 \pm 14.7 \text{ mJy}$) in the TGSS ADR, but not in any of the other large scale surveys. The noise in the VLSS_r image is very high, $\sim 500 \text{ mJy beam}^{-1}$, so its absence in this survey is not very surprising. Based on the flux density upper limit from NVSS, we calculate a spectral index of less than -2.23 between 150 MHz and 1.4 GHz . Hence, we consider this source to be a strong candidate. A UKIDSS source with a *K*-band magnitude of 17.4 is located 0.8 arcsec from the TGSS ADR location, and is a possible counterpart of the radio source.

3.8 3FGL J1925.4+1727

This candidate lies along the Galactic plane, towards the Sagittarius and Cygnus arms. It appears to be partially resolved in the TGSS ADR, with $S_{\text{t}} = 74.7 \pm 10.4 \text{ mJy}$. The non-detection in NVSS implies a spectral index of less than -1.52 between 150 MHz and 1.4 GHz . A resolved source at 327 MHz is also reported at this position with a flux density of $71 \pm 8 \text{ mJy}$ (Taylor et al. 1996). This

candidate may be a flat spectrum object at MHz frequencies and thus consider this source to be a weak candidate. There is a stellar source with a *R*-band magnitude of 17.6 located within 2.5 arcsec from the TGSS ADR location, and could be the optical counterpart of the radio source.

3.9 3FGL J1949.3+2433

This source has a total flux density of 160.4 ± 11.4 mJy in the TGSS ADR at 150 MHz and appears to be partially resolved. It is also detected in the NVSS at 1.4 GHz (5.1 ± 0.5 mJy) and the WSRT Galactic plane survey at 327 MHz (31 ± 4 mJy), but not in the VLSS_r. The 75 MHz image cutout from the latter survey is rather noisy, which appears to be the reason for the non-detection. A fit to the flux densities from these different catalogues gives a spectral index of -1.51 ± 0.15 . Considering the modest steepness of the spectrum together with the partially resolved nature of the source in the TGSS ADR, we claim that this source is a weak candidate. A bright near-infrared source catalogued in 2MASS lies 1.2 arcsec offset from the TGSS ADR source. It has a *J*-band magnitude of 16.2, and is a possible counterpart of the radio source.

3.10 3FGL J2028.5+4040c

This candidate lies near Cygnus OB2 star-forming region. The total flux density in the TGSS ADR is 389.7 ± 20.2 . The source is not seen in the VLSS_r image cutout, but the 74 MHz data are rather noisy in this Galactic plane direction. A point source is detected in the NVSS (12.8 ± 0.7 mJy), the WENSS (218 ± 9.4 mJy) and the WSRT Galactic plane survey (126 ± 7 mJy). Setia Gunawan et al. (2003) report 144 ± 7 mJy and 62 ± 9 mJy at 350 MHz and 1.4 GHz, respectively, while Wendker, Higgs & Landecker (1991) measure a 1.4 GHz flux density of 64 ± 3 mJy. It appears likely that this is a variable radio source.

The steep spectrum calculated between TGSS ADR and NVSS, -1.57 , could be a variability artefact, due to the fact that these measurements are taken at different epochs. In this case, the gamma-rays could originate from a variable AGN seen through the Galactic plane (e.g. Tsutsumi et al. 1995). Alternatively, this could be a neutron star in a Be binary system such as LSI+61°303, PSR B1259–63 or PSR J2032+4127 (Lyne et al. 2015).

There is a stellar source catalogued in Wide-Field Infrared Survey Explorer (*WISE*), Two Micron All-Sky Survey (2MASS), and Sloan Digital Sky Survey (SDSS) 5.2 arcsec offset from the TGSS ADR source. From the optical and infrared photometry we estimate its distance to be ~ 100 pc, and the spectral type to be M, assuming that it is on the main sequence. Another optical source in the vicinity is a galaxy in SDSS that is 3.6 arcsec offset from the radio source. We reject both these sources as possible counterparts to the TGSS ADR source, given that their offset distances are much larger than the uncertainty in the TGSS ADR source location.

3.11 3FGL 2210.1+5925

The TGSS ADR source ($S_{\text{t}} = 158.7 \pm 5.0$) lies just south of an extended, catalogued NVSS source (3.1 ± 0.5 mJy), located 4.5 arcsec away. At the TGSS ADR source position, the NVSS peak flux density is 2.5 mJy beam⁻¹. There is a WENSS 327 MHz source (57 ± 5.1 mJy) and weak VLSS_r emission at this location (360 ± 150 mJy beam⁻¹). A fit using all of these detections gives a spectral index of -1.71 ± 0.17 . There are no other counterparts within 3 arcsec of the TGSS ADR source in the Vizier data base.

4 DISCUSSION AND CONCLUSIONS

Pulsars are ultrastep spectrum radio sources with power-law spectra extending (typically) from 100 MHz to several GHz, with slopes $\alpha = -1.8 \pm 0.2$ (where $S_{\nu} \propto \nu^{\alpha}$; Maron et al. 2000). While the *intrinsic* spectral indices may be slightly flatter (-1.4 ± 1.0 ; Bates, Lorimer & Verbiest 2013), they are still considerably steeper than the canonical $\alpha = -0.7$ slope of the extragalactic sources that dominate source counts of the radio sky. In Kimball & Ivezić (2008), fewer than 0.4 per cent of the radio sources have $\alpha < -1.8$, or less than 1 source per 140 deg². At the steep spectrum completeness limit of the TGSS ADR, we estimate that there are 1.7 steep spectrum sources per deg² (Intema et al. 2016). The only other known discrete radio class with similar spectral slopes are the luminous high redshift galaxies (HzRGs). These rare, massive, star-forming galaxies are highly sought after in their own right as they are known to be excellent tracers of protoclusters in the early universe (Miley & De Breuck 2008).

HzRGs are not known to be gamma-ray emitters. Thus, if our steep spectrum sources are pulsars, then the radio and gamma-ray properties of the sample should resemble that of the known *Fermi* pulsars. Table 1 lists some of these properties taken directly from the 3FGL catalogue. In their galactic distribution and their radio flux densities these candidates are similar to the known pulsars. By and large the gamma-ray properties of our candidates also resemble the known sample. Apart from the mode-changing pulsar PSR J2021+4026 (Stappers et al. 2014), transitional pulsars such as PSR J1023+0038 (Allafort et al. 2013), strongly glitching pulsars (e.g. Pletsch et al. 2012b), and the Crab pulsar, gamma-ray light curves do not vary. None of the candidates are variable gamma-ray sources; the variability indices in Table 1 are all within the range of the known *Fermi* pulsars (Abdo et al. 2013). Likewise, pulsars are known to have power-law spectra in gamma-rays with exponential cutoffs around a few GeV. Here we find some differences between known pulsars and our candidates. The spectral curvature values in Table 1 are distributed on the low end of the known pulsar distribution. All but two are listed in the 3FGL as having simple power-law fits, while the two candidates with the largest values of curvature are fitted with log parabolic forms. However, with some exceptions, our *Fermi* unassociated sources are not bright in gamma-rays (Sig. < 10) and thus measuring significant exponential cutoffs would be difficult in these cases. Camilo et al. (2015) have cautioned against eliminating 3FGL pulsar candidates on the basis of spectral curvature when the source is not bright in gamma-rays or the diffuse background is high.

More information is required to determine whether these compact TGSS ADR radio sources within the unassociated error ellipses are pulsars. Our positions at 150 MHz are good to only ± 2 arcsec. This is sufficient accuracy to look for X-ray and (variable) optical counterparts, and to do a blind search for pulsed gamma-ray emission from normal pulsars of the brighter candidates. However, in order to reduce the computation costs for blind searches of MSPs, we need the sub-arcsecond positions that a radio interferometer provides. Such follow-up observations have the added benefit of allowing us to reject candidates. Pulsars are unresolved while HzRGs have kpc-size extended structure that will be visible at arcsecond resolution. Likewise, the radio surveys we used for calculating the spectral indices were taken two decades ago and thus some variable sources may have been falsely identified as steep spectrum.

The current positions of the candidates are sufficient to carry out radio pulsation searches with single dishes, but we must first understand why they have been missed in the first place. Several

of our candidates are at high galactic latitudes where existing radio searches have been concentrated. Camilo et al. (2015) have noted that there remain many 3FGL unassociated sources at high galactic latitudes with strong PSR-like characteristics but for which no radio pulsations have yet been found. Radio quiet MSPs are thought to be rare so they explain this anomaly as originating from flux modulation due to interstellar scintillation, or a rapidly changing period due to the PSR being in a tight binary. Our imaging method identifies PSR candidates without regard to binary orbits, and since the 150 MHz measurements are averaged over a night's observing they can mitigate the effects of interstellar modulation somewhat. It may be that a repeated search of these 3FGL error ellipses may yield new MSPs. We note that none of our 3FGL sources are in the lists of the 3FGL sources searched at Arecibo or Parkes (Camilo et al. 2015; Cromartie et al. 2016). The situation at low galactic latitudes is less promising. The most likely explanation for the lack of detection, if these are indeed pulsars, is that the temporal broadening along the line of sight is too large. For the brighter candidates in our sample, it could be worthwhile to search at frequencies above 3 GHz where such temporal scattering effects are much reduced ($\propto \nu^{-4}$).

Summarizing, we have identified 11 compact, steep spectrum radio sources that are positionally coincident with *Fermi* 3FGL unassociated sources. We argue that these are strong pulsar candidates and we outline the necessary next steps that need to be taken to confirm or refute this hypothesis.

ACKNOWLEDGEMENTS

This research has made use of data and/or software provided by the High Energy Astrophysics Science Archive Research Center (HEASARC), which is a service of the Astrophysics Science Division at NASA/GSFC and the High Energy Astrophysics Division of the Smithsonian Astrophysical Observatory. This work has also made extensive use of the SIMBAD and VizieR data bases maintained by the Centre de Données astronomiques de Strasbourg. KPM acknowledges funding from the Hintze Foundation. DAF thanks S. Kulkarni and T. Readhead for their hospitality at Caltech while this work was being written up. HTI acknowledges financial support through the NL-SKA roadmap project funded by the NWO. The National Radio Astronomy Observatory is a facility of the National Science Foundation operated under cooperative agreement by Associated Universities, Inc.

Facilities: GMRT, *Fermi* (LAT).

REFERENCES

Abdo A. A. et al., 2013, *ApJS*, 208, 17
Acero F. et al., 2015, *ApJS*, 218, 23

- Allafort A. et al., 2013, *ApJ*, 777, L2
Bates S. D., Lorimer D. R., Verbiest J. P. W., 2013, *MNRAS*, 431, 1352
Becker R. H., White R. L., Helfand D. J., 1995, *ApJ*, 450, 559
Bock D. C.-J., Large M. I., Sadler E. M., 1999, *AJ*, 117, 1578
Camilo F. et al., 2012, *ApJ*, 746, 39
Camilo F. et al., 2015, *ApJ*, 810, 85
Caraveo P. A., 2014, *ARA&A* 52, 211
Condon J. J., Cotton W. D., Greisen E. W., Yin Q. F., Perley R. A., Taylor G. B., Broderick J. J., 1998, *AJ*, 115, 1693
Cromartie H. T. et al., 2016, *ApJ*, 819, 34
Erickson W., 1980, *BAAS*, 12, 799
Hamilton T. T., Helfand D. J., Becker R. H., 1985, *AJ*, 90, 606
Intema H. T., Jagannathan P., Mooley K. P., Frail D. A., 2016, *A&A*, preprint ([astro-ph/1603.04368](https://arxiv.org/abs/astro-ph/1603.04368))
Kimball A. E., Ivezić Ž., 2008, *AJ*, 136, 684
Lane W. M., Cotton W. D., van Velzen S., Clarke T. E., Kassim N. E., Helmboldt J. F., Lazio T. J. W., Cohen A. S., 2014, *MNRAS*, 440, 327
Lyne A. G., Stappers B. W., Keith M. J., Ray P. S., Kerr M., Camilo F., Johnson T. J., 2015, *MNRAS*, 451, 581
Maron O., Kijak J., Kramer M., Wielebinski R., 2000, *A&A*, 147, 195
Massaro F., Thompson D. J., Ferrara E. C., 2015, *A&AR*, 24, 2
Miley G., De Breuck C., 2008, *A&AR*, 5, 67
Navarro J., de Bruyn A. G., Frail D. A., Kulkarni S. R., Lyne A. G., 1995, *ApJ*, 455, L55
Petrov L., Mahony E. K., Edwards P. G., Sadler E. M., Schinzel F. K., McConnell D., 2013, *MNRAS*, 432, 1294
Pletsch H. J. et al., 2012a, *Science*, 338, 1314
Pletsch H. J. et al., 2012b, *ApJ*, 755, L20
Ransom S. M. et al., 2011, *ApJ*, 727, L16
Rengelink R. B., Tang Y., de Bruyn A. G., Miley G. K., Bremer M. N., Roettgering H. J. A., Bremer M. A. R., 1997, *A&AS*, 124, 259
Rickard J. J., Cronyn W. M., 1979, *ApJ*, 228, 755
Schinzel F. K., Petrov L., Taylor G. B., Mahony E. K., Edwards P. G., Kovalev Y. Y., 2015, *ApJS*, 217, 4
Setia Gunawan D. Y. A., de Bruyn A. G., van der Hucht K. A., Williams P. M., 2003, *ApJS*, 149, 123
Stappers B. W. et al., 2014, *ApJ*, 790, 39
Stroh M. C., Falcone A. D., 2013, *ApJS*, 207, 28
Strom R. G., 1987, *ApJ*, 319, L103
Taylor M. B., 2005, in Shopbell P., Britton M., Ebert R., eds, *ASP Conf. Ser. Vol. 347, Astronomical Data Analysis Software and Systems XIV*. Astron. Soc. Pac., San Francisco, p. 29
Taylor A. R., Goss W. M., Coleman P. H., van Leeuwen J., Wallace B. J., 1996, *ApJS*, 107, 239
Tsutsumi T., Gregory P. C., Duric N., Taylor A. R., 1995, *AJ*, 110, 238
Wendker H. J., Higgs L. A., Landecker T. L., 1991, *A&A*, 241, 551

This paper has been typeset from a $\text{\TeX}/\text{\LaTeX}$ file prepared by the author.